Journal of Solid State Chemistry **147,** 618–623 (1999)
Article ID jssc.1999.8425, available online at http://www.idealibrary.com on IDEAL®

Magnetic Properties of Ordered Perovskites Ba_2LnIrO_6 ($Ln = $ Sm, Eu, Gd, and Yb)

Makoto Wakeshima, Daijitsu Harada, and Yukio Hinatsu

Division of Chemistry, Graduate School of Science, Hokkaido University, Sapporo 060-0810, Japan

and

Nobuyuki Masaki

Japan Atomic Energy Research Institute, Tokai-mura, Ibaraki 319-11, Japan

Received March 18, 1999; in revised form June 4, 1999; accepted June 8, 1999

Magnetic properties of ordered perovskites Ba_2LnIrO_6 ($Ln =$ Sm, Eu, Gd, and Yb) are reported. Their magnetic susceptibilities were measured from 2 to 350 K. The ^{151}Eu Mössbauer spectrum of Ba_2EuIrO_6 and the electronic paramagnetic resonance (EPR) spectrum of Ba_2GdIrO_6 were measured at room temperature. Ba_2EuIrO_6 and Ba_2SmIrO_6 show Van Vleck paramagnetism. A spin–orbit coupling constant of the Eu^{3+} ion is determined to be 364 cm^{-1}. The Mössbauer spectrum of Ba_2EuIrO_6 shows that the Eu ion is in the trivalent state, and the symmetry of the Eu site is slightly distorted from an octahedral symmetry because of the existence of a quadrupole interaction. The magnetic susceptibilities of Ba_2GdIrO_6 and Ba_2YbIrO_6 follow the Curie law and the crystal field splitting of the Yb^{3+} ion is calculated. The g value of the Gd^{3+} ion in Ba_2GdIrO_6 is determined to be 1.99 and Gd^{3+} is very slightly affected by the crystal field from the EPR measurement. © 1999 Academic Press

INTRODUCTION

Ordered perovskite-type oxides A_2LnMO_6 ($A =$ Sr, Ba; $Ln =$ lanthanide; $M = 4d$ or $5d$ transition metal) in which the Ln and M sites regularly show an interesting magnetic behavior at low temperatures. Battle *et al.* reported that Sr_2YRuO_6, Sr_2LuRuO_6, and Sr_2ErRuO_6 exhibited antiferromagnetic transitions, and their magnetic structures were determined by neutron diffractometry (1–3). Recently, Doi and Hinatsu measured magnetic susceptibilities of a series of Sr_2LnRuO_6 phases and found that these phases show a very unique and complex magnetic behavior below 40 K (4). Through magnetic studies on a series of Sr_2LnIrO_6 phases, Harada *et al.* showed that Sr_2CeIrO_6 and Sr_2TbIrO_6 are antiferromagnetic below 21 and 51 K, respectively (5). In these compounds, most of the magnetic transitions are due to the interaction between d electrons and f electrons.

We focus our attention on the ordered perovskites Ba_2LnIrO_6 ($Ln =$ lanthanide). Ramos *et al.* reported that Ba_2LnIrO_6 ($Ln =$ La, Pr, and Ho) phases are paramagnetic (6). We recently reported that the magnetic behavior of the Ir ions in Ba_2RIrO_6 ($R =$ nonmagnetic rare earth ion) could be explained by Kotani's theory (7) and that their oxidation states were pentavalent with the low spin configurations (8). In this paper, we will report the magnetic properties of Ba_2LnIrO_6 ($Ln =$ Sm, Eu, Gd, and Yb) through their magnetic susceptibilities, electron paramagnetic resonance (EPR) spectra, and ^{151}Eu Mössbauer spectrum measurements.

EXPERIMENTAL

As starting materials, barium carbonate, lanthanide sesquioxide (Ln_2O_3; $Ln =$ Sm, Eu, Gd, and Yb), and iridium metal powder were used. Their purity is higher than 99.9%. They were weighted in ratios, intimately mixed, pelletized, and calcined in air at 1173 K for 6 h. The products were heated in air at 1473 K for several days with regrinding and repelletizing.

The magnetic susceptibility was measured in the temperature range between 2 and 350 K in a magnetic field of 0.1 T with a SQUID magnetometer (Quantum Design, Model MPMS).

The EPR spectrum was obtained at room temperature with a JEOL 2XG spectrometer at X band frequency ($\nu \sim$ 9.1 GHz). The magnetic field was monitored with a proton NMR gaussmeter.

The ^{151}Eu Mössbauer spectrum was measured with a conventional transmissional Mössbauer spectrometer VT-6000 (Laboratory Equipment Co., Japan) at room temperature. The spectrometer was calibrated using α-iron at room

0022-4596/99 $30.00

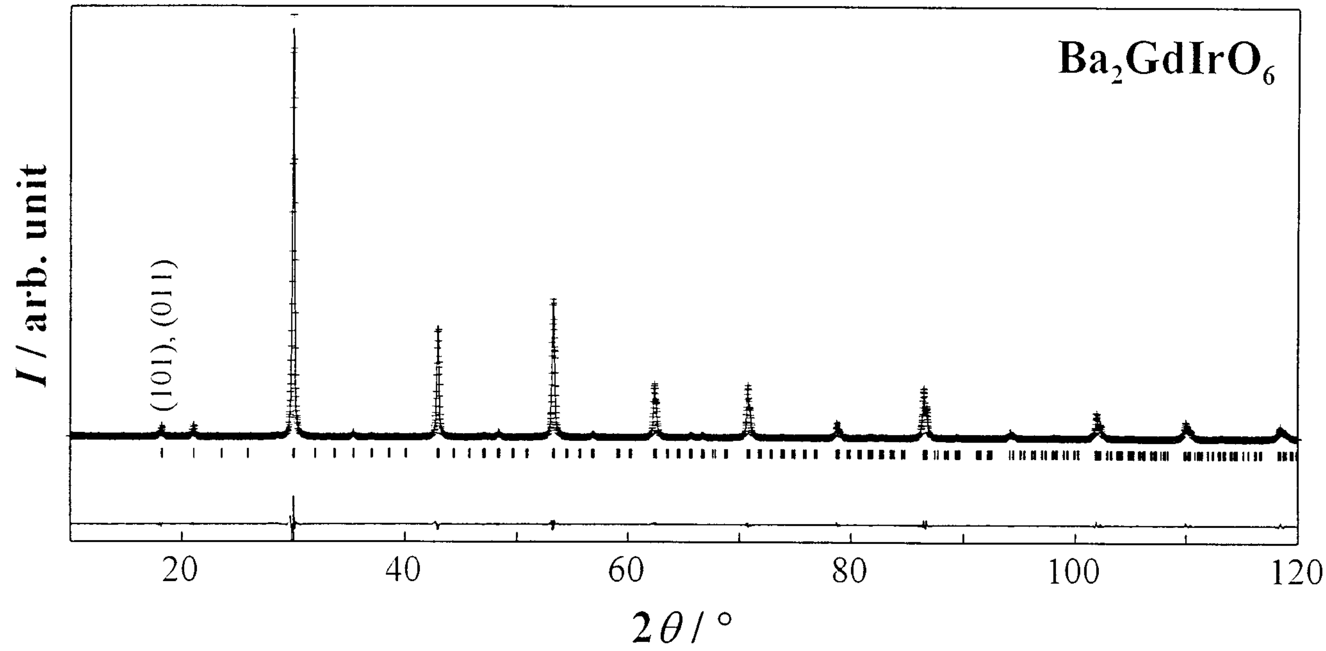

FIG. 1. X-ray diffraction profiles for Ba_2GdIrO_6. The calculated and observed diffraction profile is shown on the top solid line and the cross markers, respectively. The vertical marks in the middle show positions calculated for Bragg reflections. The bottom trace is a plot of the difference between calculated and observed intensities.

temperature and the isomer shift was determined relative to the shift of europium trifluoride (EuF_3).

RESULTS AND DISCUSSION

All the reaction products Ba_2LnIrO_6 were black in color and were formed as a single phase with a perovskite-type structure. Their X-ray diffraction patterns were indexed on a monoclinic unit cell (space group $P2_1/n$), and their structural analyses using the Rietveld method show that the Ln^{3+} and Ir^{5+} ions are arranged alternatively and that they have a rock salt sublattice. For example, the result of X-ray diffraction pattern fitting for Ba_2GdIrO_6 is shown in Fig. 1. The diffraction profile shows the existence of the superlattice reflection at $2\theta \approx 19°$ caused by the ordered arrangement between the Gd and Ir ions.

The results of the magnetic susceptibility measurements for Ba_2LnIrO_6 (Ln = Sm, Eu, Gd, and Yb) show that all compounds are paramagnetic in the temperature range between 2 and 350 K. Both Ln^{3+} and Ir^{5+} ions contribute to the paramagnetic behavior of these compounds. To determine the magnetic behavior of Ln^{3+} ion in solids, we subtracted the magnetic susceptibilities of Ba_2LuIrO_6 (the Lu^{3+} is diamagnetic) from those of Ba_2LnIrO_6.

Ba_2SmIrO_2

Figure 2 shows the temperature dependence of the magnetic susceptibilities of Sm^{3+} ion in Ba_2SmIrO_6. The ground state of the Sm^{3+} ion is $^6H_{5/2}$. At low temperatures, only the magnetic $^6H_{5/2}$ ground multiplet is populated. However, since the energy differences between the ground state and the excited states ^6H_J ($J = 7/2, 9/2, \ldots, 13/2$) are not so large compared to thermal energy k_BT, we must take the population to the excited states into consideration in the calculation of the magnetic susceptibilities at high temperatures. According to the Van Vleck theory, the molar magnetic susceptibility of the Sm^{3+} ion is given by (9)

$$\chi(Sm^{3+}) = \frac{N_A\mu_B^2/3k_B}{\delta T}\,\frac{2.14\delta + 3.67 + (42.9\delta + 0.82)e^{-7\delta} + (142\delta - 0.33)e^{-16\delta} + \cdots}{3 + 4e^{-7\delta} + 5e^{-16\delta} + \cdots}, \qquad [1]$$

where N_A and μ_B are the Avogadro number and the Bohr magneton, respectively. The parameter $\delta = \lambda/k_BT$ is 1/55 of the ratio of the overall multiplet width (the spin–orbit coupling constant, λ) and the thermal energy (k_BT). The best fit of Eq. [1] to the experimental data is shown in Fig. 2 with a solid line, which gives $\lambda = 422\ cm^{-1}$. The energy difference between the ground state $^6H_{5/2}$ and the first excited state $^6H_{7/2}$ is determined to be $1477\ cm^{-1}$, which is near to the Van Vleck's theoretical value ($1540\ cm^{-1}$) (9).

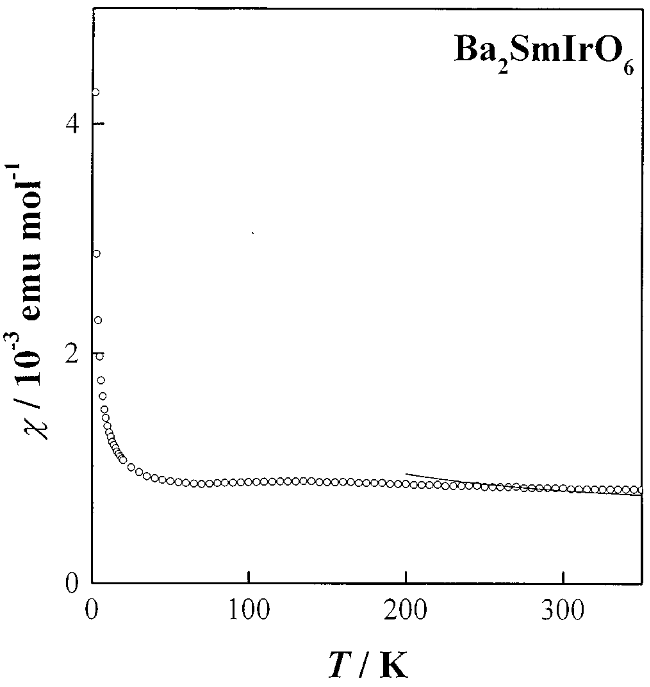

FIG. 2. Temperature dependence of the magnetic susceptibility of Sm^{3+} ion in Ba_2SmIrO_6.

Ba_2EuIrO_6

Figure 3 shows magnetic susceptibilities of Eu^{3+} ion in Ba_2EuIrO_6 as a function of temperature. The susceptibilities increase with decreasing temperature for temperatures $\geq$100 K and become constant below 100 K. The shape of this curve is characteristic of a Van Vleck paramagnet. The ground state $^7F_0$ of Eu^{3+} is nonmagnetic, and the excited states ^7F_J ($J = 1, 2, \ldots, 6$) are close enough to give energy differences comparable to k_BT at room temperature. The excitation to upper state affects sufficiently the magnetic susceptibility at room temperature. Thus, the molar magnetic susceptibility for Eu^{3+} can be written by (9)

$$\chi(Eu^{3+}) = \frac{N_A\mu_B^2/3k_B}{\gamma T} \frac{24 + (13.5\gamma - 1.5)e^{-\gamma} + (67.5\gamma - 2.5)e^{-3\gamma} + (189\gamma - 3.5)e^{-6\gamma} + \cdots}{1 + 3e^{-\gamma} + 5e^{-3\gamma} + 7e^{-6\gamma} + \cdots}, \qquad [2]$$

where $\gamma = \lambda/k_BT$ is 1/21 of the ratio the overall multiplet width to k_BT. The magnetic susceptibilities calculated by using Eq. [2] are fitted to the measured susceptibilities in the range of 10 to 350 K, as shown in Fig. 3 with a solid line. The spin–orbit coupling constant λ of Eu^{3+}, which is the energy-level difference between the ground state $^7F_0$ and the first excited state $^7F_1$, is determined to be 364 cm^{-1} for Ba_2EuIrO_6 and is in good agreement with the previously reported values in other compounds containing Eu^{3+}, for example, 352 cm^{-1} ($Cs_2NaEuCl_6$) obtained from the luminescence spectra (10) and 365 cm^{-1} (Eu_2BaZnO_5) from the magnetic susceptibility (11).

The ^{151}Eu Mössbauer spectrum of Ba_2EuIrO_6 measured at room temperature is shown in Fig. 4. For comparison, the spectrum of Sr_2EuIrO_6 is shown in the same figure. The Eu site has the point symmetry $\bar{1}$, which is distorted from an octahedral symmetry $m\bar{3}m$. Then, the electric field gradient exists and the quadrupole Hamiltonian is given by

$$H_Q = \frac{e^2qQ}{4I(2I-1)}[3I_z^2 - I(I+1) + \eta(I_x^2 - I_y^2)], \qquad [3]$$

where Q is the quadrupole moment, $eq = V_{zz}$, I is the nuclear spin, and $\eta = (V_{xx} - V_{yy})/V_{zz}$ (V_{ii} is the electric field gradient tensor). Actually, the spectrum exhibited a slightly asymmetric line. It is impossible to fit such a spectrum with a single Lorentzian line because of the distortion due to the quadrupole interaction. The asymmetry parameter η is not equal to zero at the Eu site, because the point symmetry is not axially symmetric. Figure 4 shows 12 possible transitions due to a quadrupole interaction. The observed spectra were fitted with the 12 Lorentzian lines. The positions of the lines depend on the isomer shift δ, the quadrupole coupling constant eQ_gV_{zz}, and the ratio $R_Q = Q_e/Q_g$ of the excited and ground state quadrupole moments.

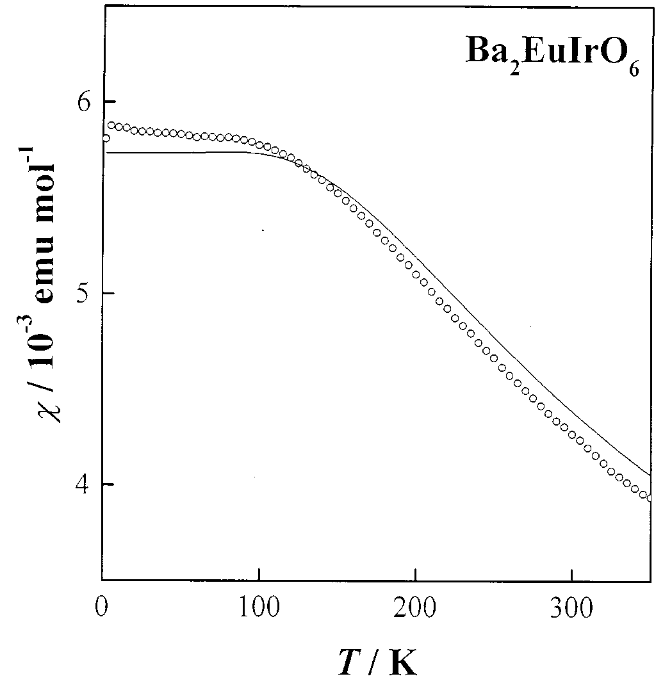

FIG. 3. Temperature dependence of the magnetic susceptibility of Eu^{3+} ion in Ba_2EuIrO_6.

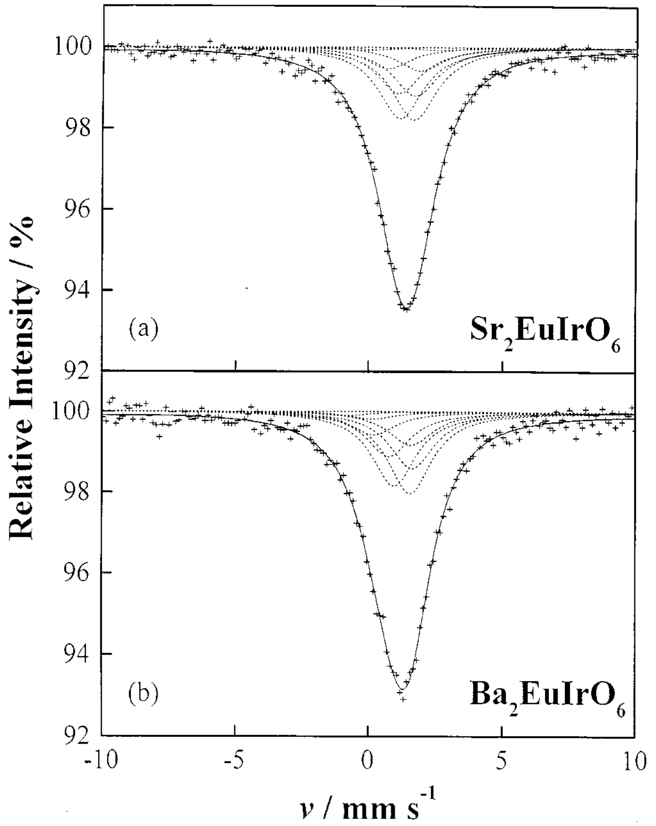

FIG. 4. ^{151}Eu Mössbauer spectra of Sr_2EuIrO_6 (a) and Ba_2EuIrO_6 (b) measured at room temperature.

Table 1 lists the ^{151}Eu Mössbauer parameters determined for Sr_2EuIrO_6 and Ba_2EuIrO_6. The isomer shifts δ for Sr_2EuIrO_6 and Ba_2EuIrO_6 are 1.39 and 1.18 mm/s, respectively, which confirms that the Eu ions are in the trivalent state in both compounds. The average Eu–O bond lengths in the Sr_2EuIrO_6 and Ba_2EuIrO_6 are 2.215 and 2.246 Å, respectively. These results coincide with the reported correlation between the isomer shifts of Eu^{3+} ion and the Eu–O bond lengths in the Eu^{3+} compounds (12, 13); i.e., the isomer shifts of Eu^{3+} ion decrease with increasing Eu–O bond lengths. The asymmetry parameters η of Sr_2EuIrO_6 and Ba_2EuIrO_6 are determined to be 0.75 and 0.37, respectively. Compared with the value of η for Sr_2EuIrO_6, a lower value of η is obtained for Ba_2EuIrO_6, which is in good agreement with the results from the crystal structure measurements.

TABLE 1
^{151}Eu Mössbauer Parameters of Sr_2EuIrO_6 and Ba_2EuIrO_6 at Room Temperature[a]

	Sr_2EuIrO_6	Ba_2EuIrO_6
δ (mm s^{-1})	1.40	1.18
$eV_{zz}Q_g$ (mm s^{-1})	3.39	4.92
η	0.75	0.37

[a] δ, $eV_{zz}Q_g$, and η are isomer shift, quadrupole coupling constant, and asymmetry parameter, respectively.

Ba_2GdIrO_6

The temperature dependence of the reciprocal magnetic susceptibilities of Gd^{3+} ion in Ba_2GdIrO_6 is shown in Fig. 5. The reciprocal susceptibilities χ^{-1} increase linearly with temperature and obeys the Curie law. The effective magnetic moment of the Gd^{3+} ion is determined to be 7.63 μ_B. This value is near the theoretical magnetic moment ($\mu_{eff} = 7.94\ \mu_B$) of the free Gd^{3+} ion.

Figure 6 shows the X-band EPR spectrum for Ba_2GdIrO_6 measured at room temperature. For comparison, the spectrum for Sr_2GdIrO_6 is shown in the same figure. For Ba_2GdIrO_6, a single broad spectrum, centered at 325.9 mT (therefore $g = 1.99$) with linewidth 78.8 mT, was measured, which is ascribable to the Gd^{3+} ion. The EPR spectrum for the Ir^{5+} (d^4) is seldom observed because of the singlet ground state in an octahedral ligand field. In fact, no EPR spectrum for Ba_2LuIrO_6 is measured. The EPR spectrum for Sr_2GdIrO_6 shows a very broad line associated with the Gd^{3+} ion. This spectrum means that the ligand environment of the Gd^{3+} ion in Sr_2GdIrO_6 is considerably distorted from octahedral symmetry. If the ground state of the

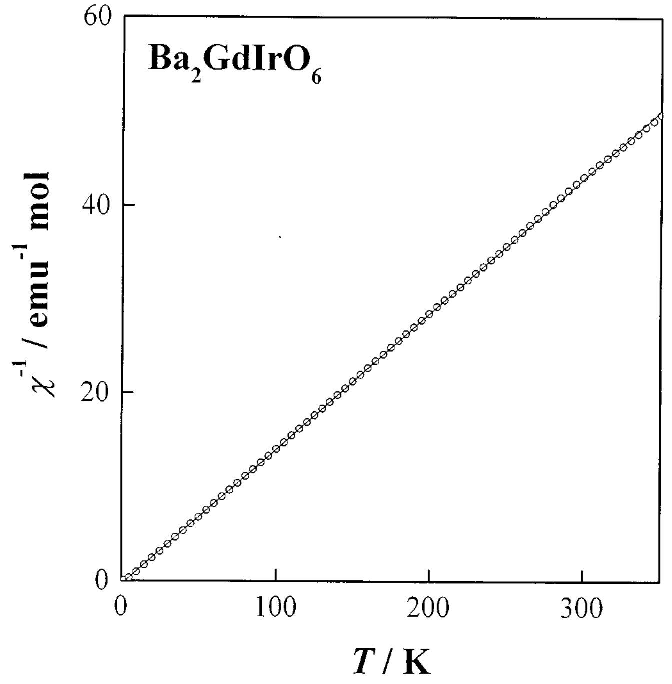

FIG. 5. Temperature dependence of the reciprocal magnetic susceptibility of Gd^{3+} ion in Ba_2GdIrO_6.

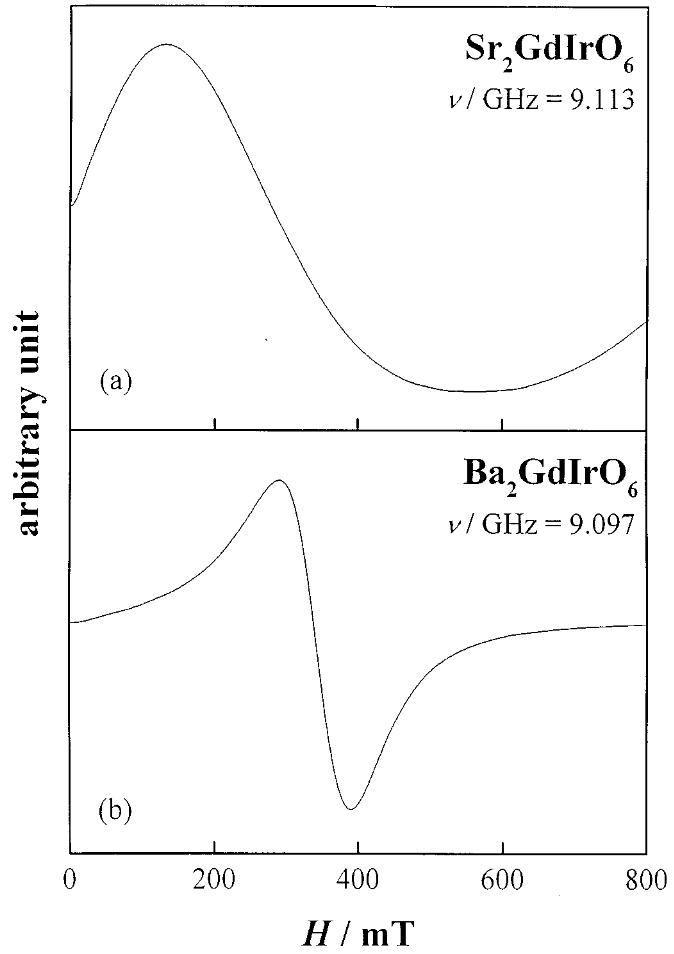

FIG. 6. EPR spectra of Sr_2GdIrO_6 (a) and Ba_2GdIrO_6 (b) at room temperature.

rare earth ions with a half-filled *f* shell such as Eu^{2+}, Gd^{3+}, or Tb^{4+} is a pure $^8S_{7/2}$ state, the *g*-value is 2.00 for the EPR measurement because of no interactions except for a Zeeman interaction. For example, Hinatsu reported that the *g* value of the Tb^{4+} ions was very close to the theoretical value ($g = 2.00$) in tetravalent terbium perovskites, $SrTbO_3$ and $BaTbO_3$ (14). The *g* value ($g = 1.99$) of Ba_2GdIrO_6 obtained from this EPR measurement is in good agreement with the theoretical value.

Ba_2YbIrO_6

The temperature dependence of the reciprocal magnetic susceptibility of Yb^{3+} ion in Ba_2YbIrO_6 is shown in Fig. 7. The ground state $^2F_{7/2}$ of Yb^{3+} is split into two doublets (Γ_6 and Γ_7) and one quartet (Γ_8) in the octahedral symmetry. One expects that the ground state is Γ_6 and that the first and second excited states are Γ_7 and Γ_8, respectively, analogous with results for $Cs_2NaYbCl_6$ (15). The susceptibility of the Yb^{3+} ion is then given by

$$\chi(\mathrm{Yb}^{3+}) = \frac{N_A g_J^2 \mu_B^2 J(J+1)}{3k_B T}\left(98 + 260e^{-\Delta_{68}/k_BT} + 162e^{-\Delta_{67}/k_BT} + \frac{432k_BT}{\Delta_{68}-\Delta_{67}}\left(e^{-\Delta_{67}/k_BT} - e^{-\Delta_{68}/k_BT}\right) + \frac{560k_BT}{\Delta_{68}}\left(1 - e^{-\Delta_{68}/k_BT}\right)\right)\Bigg/ 378\left(1 + 2e^{-\Delta_{68}/k_BT} + e^{-\Delta_{67}/k_BT}\right), \quad [4]$$

where Δ_{68} is the energy difference between the Γ_6 and Γ_8 levels and Δ_{67} is that between the Γ_6 and Γ_7 levels. By fitting this equation to the experimental magnetic susceptibility, the effective magnetic moment for Yb^{3+} is obtained to be 4.54 μ_B, which agrees with the theoretical value ($\mu_{eff} = 4.54$ μ_B). The calculated energy differences Δ_{68} and Δ_{67} are 430 and 1240 cm^{-1}, respectively. These values are larger than those of $Cs_2NaYbCl_6$ (Δ_{68} and Δ_{67} are 271 and 580 cm^{-1}, respectively) (16). Since the effect of the ligand field of the O^{2-} ions is larger than that by the Cl^- ions, the energy splitting for Ba_2YbIrO_6 should be larger than that for $Cs_2NaYbCl_6$. The energy splitting for Ba_2YbIrO_6 is slightly larger than that for Ba_2YbNbO_6 (Δ_{68} and Δ_{67} are 368 and 1058 cm^{-1}, respectively).

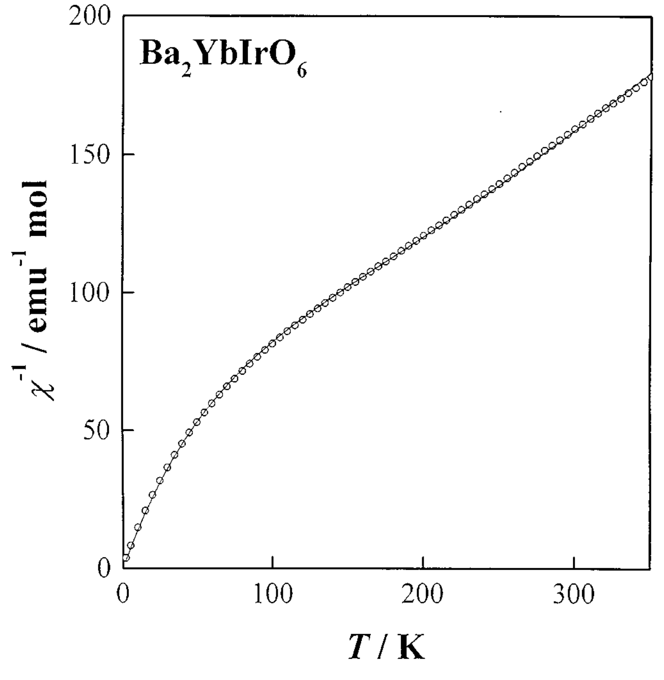

FIG. 7. Temperature dependence of the reciprocal magnetic susceptibility of Yb^{3+} ion in Ba_2YbIrO_6.

REFERENCES

1. P. D. Battle and W. J. Macklin, *J Solid State Chem.* **52,** 138 (1984).
2. P. D. Battle and C. W. Jones, *J. Solid State Chem.* **78,** 108 (1989).
3. P. D. Battle, C. W. Jones, and F. Studer, *J. Solid State Chem.* **90,** 302 (1991).
4. Y. Doi and Y. Hinatsu, *J. Phys.: Condens. Matter* **11,** 4813 (1999).
5. D. Harada, M. Wakeshima, and Y. Hinatsu, *J. Solid State Chem.* **145,** 256 (1999).
6. E. M. Ramos, I. Alvarez, R. Saéz-Puche, M. L. Veiga, and C. Pico, *J. Alloys Compound.* **225,** 212 (1995).
7. M. Kotani, *Prog. Theor. Phys. Suppl.* **14,** 1 (1960).
8. M. Wakeshima, D. Harada, and Y. Hinatsu, *J. Alloys Compound.* **287,** 130 (1999).
9. J. H. Van Vleck, "Theory of Electric and Magnetic Susceptibilities." Clarendon, Oxford, 1932.
10. C. D. Flint and F. L. Stewart-Darling, *Mol. Phys.* **44,** 61 (1981).
11. G. F. Goya, R. C. Mercader, M. T. Causa, and M. Tovar, *J. Phys.* (*Condens. Matter*) **8,** 8607 (1996).
12. S. Tanaka, K. Hirano, and N. Soda, *J. Non-Cryst. Solids* **113,** 178 (1989).
13. M. Saeki, M. Nakada, N. M. Masaki, and A. Nakamura, "Conference Proceedings, ICAME-95," Vol. 50. p. 119. Italian Physical Society, 1996.
14. Y. Hinatsu, *J. Solid State Chem.* **100,** 136 (1992).
15. B. D. Dunlap and G. K. Shenoy, *Phys Rev. B* **12,** 2716 (1975).
16. K. Henmi and Y. Hinatsu, *J. Solid State Chem*, in press.